DIAGNOSTYKA, 2024, Vol. 25, No. 2

e-ISSN 2449-5220
DOI: 10.29354/diag/188467

FAULT DIAGNOSIS ALGORITHM OF ELECTRIC VEHICLE GEARBOX BASED ON SDEA-BI GRU

Linlin ZHAO * , **Tao WU**

College of Intelligent Engineering Technology, Jiangsu Vocational College of Finance & Economics, Huaian 223003, China
* Corresponding author, e-mail: zhaolinlin108@126.com

Abstract

This paper suggests a hybrid method that combines the strengths of a bidirectional gated recurrent unit with a stacked denoising autoencoder to enhance the precision and effectiveness of diagnosing transmission faults in electric vehicles. The bidirectional gated recurrent unit makes advantage of these deep features for efficient fault pattern identification and classification. The results revealed that the hybrid algorithm had the best feature extraction ability for gear fault signals, and the signal features extracted by the algorithm were more concentrated and crossed each other less. The neurons in the hidden layer of the stacked denoising autoencoder was 180, and the number of neurons in the bidirectional gated recurrent unit was 160, and the hybrid algorithm performed best when the neurons in the hidden layer was 180 and the neurons in the bidirectional gated recurrent unit was 160. The hybrid algorithm performed best when the number of neurons was 160. The hybrid algorithm had the highest diagnostic accuracy for the faults, with the highest diagnostic accuracy of 97.98% in the balanced samples and 94.86% in the unbalanced samples. The hybrid algorithm constructed in the study effectively improves the diagnostic accuracy of transmission gear faults in electric vehicles..

Keywords: transmission, electric vehicle, SDEA, Bi-GRU, gear failure

1. INTRODUCTION

Electric vehicles have drawn a lot of attention as an alternative form of transportation in light of the growing severity of the energy crisis and environmental pollution. Because of their clean and efficient energy use, electric vehicles have also emerged as a key trend in the development of the contemporary automotive industry [1]. However, electric vehicle as a complex mechatronic product, in which the stability and safety of the electric gearbox, as a key component connecting the motor and the traveling system, are critical to the overall vehicle performance [2]. Accurate and timely identification of possible transmission defects has become a must to guarantee the regular functioning of electric vehicles, and fault diagnosis is crucial for enhancing the operational safety and dependability of electric vehicles [3]. Currently, fault diagnosis techniques for electric vehicle transmission mainly focus on traditional methods such as vibration and sound analysis, but these methods usually require specialized personnel to operate, and the diagnostic accuracy is insufficient in the changing operating environment [4]. The use of SDEA and bidirectional gated recurrent unit (Bi-GRU) in the proposed algorithm enhances the accuracy and efficiency of fault diagnosis in electric vehicle transmission. The study proposes a composite algorithm based on stacked denoising autoencoder (SDEA) and Bi-GRU to improve the efficiency and accuracy of fault diagnosis of electric vehicle transmission using machine learning-based methods. The study uses SDEA for feature extraction. SDEA learns deep feature expressions from complex transmission signals by introducing noise to resist overfitting. These features are then combined with an advanced Bi-GRU model for fault mode identification and classification. Bi-GRU captures before-and-after information in time-series data through its bi-directional structure, making the fault diagnosis both accurate and adaptable.

The study combines Bi-GRU with SDEA to establish a hybrid SDEA-Bi-GRU model for gear fault diagnosis of gearboxes for electric vehicle transmissions. The research's primary contribution is the suggestion of a novel gear fault diagnosis model for electric vehicle transmission, which offers a fresh approach to fault diagnosis of electric vehicle. The study will consist of four parts: first, a review of the current research on fault diagnosis, SDEA, and Bi-GRU for electric vehicle transmission. Second, research on electric vehicle transmission diagnosis based on the SDEA-Bi-GRU model. Third,

Received 2024-01-17; Accepted 2024-05-09; Available online 2024-05-28

experimental validation of the SDEA-Bi-GRU model. And finally, an overview of the research

2. RELATED WORKS

Electric vehicle is currently the most compatible low-carbon and energy-saving vehicle type. To improve the effectiveness of battery fault diagnosis for electric vehicles, Li et al. proposed a new battery fault diagnosis method by combining a long and short-term memory recurrent neural network and an equivalent circuit model. The results showed that the method can achieve accurate diagnosis of potential battery faults and precise localization of thermal runaway batteries [5]. In order to prevent the damage caused by over discharge of lithium-ion batteries, Gan et al. proposed a two-layer over discharge fault diagnosis strategy based on machine learning. The first layer detected over discharge by comparing the cell voltage and cutoff voltage, while the second layer used a limit gradient boosting algorithm for previous over discharge detection. The results indicated that their proposed method has good results [6]. In order to diagnose switched reluctance motor bearing faults in electric vehicle power systems under variable speed conditions, Wang X et al. proposed a multi-sensor data fusion method. The method fused synchronously sampled current and vibration signals to estimate the cumulative rotor angle. The results demonstrated that the method does not require an additional tachometer and can be used for online fault diagnosis of switched reluctance motors under variable speed conditions [7]. To protect the safe operation of electric vehicle batteries, Long et al. proposed a model-based fault diagnosis scheme for current and voltage sensors. By comparing the difference between the true state of charge and the estimated state of charge, the occurrence of faults was determined and faulty sensors were isolated. The results showed that the method can effectively diagnose battery faults [8]. To overcome the challenges of battery fault diagnosis for electric vehicles, reduce the dependence on the amount of data and improve the diagnostic accuracy and speed, Deng et al. proposed a multi-classification support vector machine (SVM) based fault diagnosis method. The results revealed that the method improved the training speed and accuracy and achieved satisfactory results in battery fault diagnosis of electric vehicles with small sample training set [9].

Both SDEA and Bi-GRU are one kind of deep learning networks. To solve the problem of SDAE's ability to extract bearing fault feature information under multiple operating conditions and strong noise, Jia et al. proposed a bearing health monitoring and fault diagnosis model based on variational mode decomposition, continuous wavelet transform and sparrow search algorithm optimized for SDAE. The outcomes revealed that the model outperforms other methods in terms of diagnostic accuracy, generalization performance and noise immunity [10]. To analyze the fault diagnosis method for rolling bearings, Che et al. addressed a SDEAFD model based on convolutional neural network (CNN). The model can denoise and dimensionalize the raw vibration signal data. The outcomes revealed that the model in improved the accuracy by 3%-13% over the traditional model and a single deep learning model [11]. A approach based on data augmentation and Bi-GRU was proposed by Fu B et al. The method utilized the principal factor correlation index to select features and used Mixup technique to enhance the data. The approach enhanced the model's resilience and capacity for generalization while maintaining a high level of prediction accuracy, according to the findings [12]. To solve the category imbalance problem, A weakly supervised learning-based classification technique was presented by Liu H et al. The method employed bi-directional gated recursive units to construct the fault diagnosis model, and proposed a new weighted cross-entropy function as the loss function to reduce the effect of noise. The method's efficacy and superiority were demonstrated by the experimental results [13].

In summary, fault detection of electric vehicle components is a current research focus. However, most research has been centered on automotive battery fault detection, with fewer studies on other key components. The gearbox is a crucial component of an automobile. Any failure of this component can directly impact the use of the automobile. Therefore, this study aims to detect faults in the electric vehicle transmission system. Commonly used fault detection methods include SDEA and Bi-GRU, but each has its own shortcomings. This study proposes to combine the two methods for fault detection in the gear system of electric vehicle transmission

3. FAULT DIAGNOSIS OF ELECTRIC VEHICLE TRANSMISSION BASED ON SDEA-BI-GRU MODELING

Gearbox gear failure is one of the most common failures in electric vehicles. Section 3 mainly focuses on the study of diagnostic methods for transmission gear failure in electric vehicles. And it is developed in two directions, the first part is the SDEA-Bi-GRU hybrid network study, and the second part is the gear fault diagnosis based on SDEA-Bi-GRU

3.1. SDEA-Bi-GRU Hybrid Networks

SDEA is a deep learning model that performs feature learning and noise reduction by stacking multiple layers of self-encoders [14-15]. Self-encoder is an unsupervised learning model that encodes and decodes the input data and learns a low-dimensional representation of the input data by minimizing the reconstruction error [16]. Stacked auto-encoders, on the other hand, stack multiple auto-encoders together, with the hidden layer of each auto-encoder serving as the input to the next autoencoder. And Figure 1 depicts the particular structure.

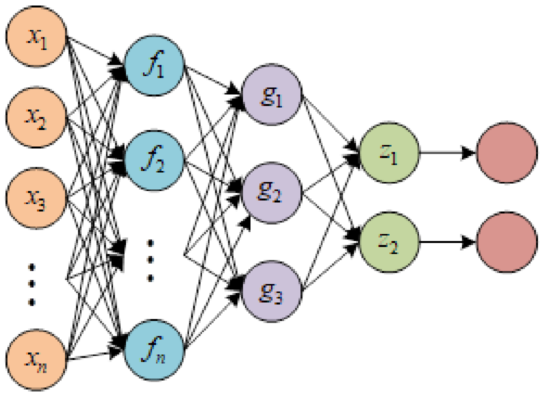

Fig. 1. SDEA network structure

In stacked noise-reducing self-coding networks, each self-encoder introduces noise to make the input data more robust, which forces the model to learn more useful and abstract features. Usually Gaussian noise or randomly interrupted input data is used as noise. Pre-training and fine-tuning are the two phases of the SDEA network training process. In the pre-training phase, signal-to-noise samples with additional noise are fed into the SDEA and mapped to the hidden layer in equation (1).

$$y = f_\theta(\tilde{x}) = s(W\tilde{x} + b) \tag{1}$$

In equation (1), $\tilde{x}$ denotes the input and $f_\theta(\square)$ denotes the encoding function. WA denotes the encoding weights and b denotes the bias. s denotes the mapping function, θ denotes the set parameters and y denotes the output. The mapping result is subsequently decoded and reconstructed in equation (2).

$$\hat{x} = g_{\theta_1}(y) = S(W_1 y + b_1) \tag{2}$$

In equation (2), $g_{\theta_1}(y)$ denotes the decoding function and W_1 denotes the decoding weights. b_1 denotes the decoding bias, S denotes the decoding mapping function, and θ_1 denotes the decoding set parameters. The fine-tuning part means that the weights in the pre-training are used as initial parameters to adjust the parameters of SDEA, and the fine-tuning of SDEA is a supervised learning process. Recurrent neural network (RNN) is a type of traditional neural network, but traditional neural networks are not able to correlate information while processing it. Therefore, scholars proposed RNN, in common RNN, a neuron needs to receive the information processed is more complex. At the current moment t, the neuron needs to receive not only the input x_t, but also the state h_{t-1} of the previous moment, as shown in equation (3).

$$h_t = f(s_t) = f(Ux_t + Wh_{t-1}) \tag{3}$$

In equation (3), f denotes the activation function, h_t denotes the state of the hidden unit at the t moment, and U denotes the weight matrix. Gated recurrent unit (GRU) is a type of RNN unit, which has good results when dealing with sequential data [17]. GRU is improved on long short-term memory network (LSTM). GRU adds an update gate and a reset gate to the network. The update gate controls how the network stores data and ignores information from prior inputs, while the reset gate controls how the network merges data from previous inputs with the data that is currently being input [18]. The output of the update gate is shown in equation (4).

$$g_t = \sigma\left(b_g + W_g x_t + U_g h_{t-1}\right) \tag{4}$$

In equation (4), g_t denotes the update gate output and σ denotes the sigmoid activation function. x_t denotes the input data at the current moment and h_{t-1} denotes the hidden unit information output at the $t-1$ moment. The reset gate output is shown in equation (5).

$$r_t = \sigma(W_r x_t + U_r h_{t-1} + b_r) \tag{5}$$

In equation (5), r_t denotes the reset gate output. the candidate hidden state expression in the GRU is shown in equation (6).

$$\tilde{h}_t = tanh(W_{\square} x_t + U_{\square}(r_t h_{t-1}) + b_h) \tag{6}$$

In equation (6), $\tilde{h}_t$ denotes the candidate hiding state. The hidden state can be represented by equation (7).

$$h_t = g_t \bullet \tilde{h}_t + (-g_t + 1)h_{t-1} \tag{7}$$

The output of GRU is shown in equation (8).

$$y_t = \sigma(W_0 h_t) \tag{8}$$

GRU is a one-way learning model, in the learning process, the last unit of the state information is missing, and the more forward, the more serious the missing information, to address this problem, scholars introduced a two-way learning mechanism in GRU. After the introduction of the two-way learning mechanism, it is Bi-GRU. Additionally, Figure 2 depicts the network's topology.

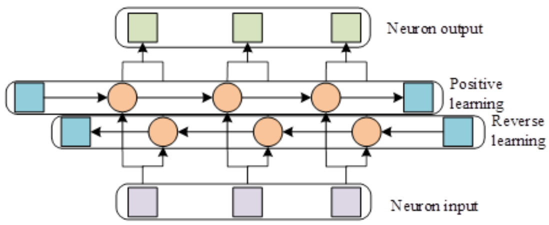

Fig. 2. Bi GRU structure

Bi-GRU uses all the information of the unit in the past and the future in a bidirectional learning mechanism to complement the features lost in the training process of the GRU. And equation (9) displays the model's output formula.

$$h_t = [\vec{h}_t \oplus \overleftarrow{h}_t] \tag{9}$$

In equation (9), $\vec{h}_t$ denotes the forward learning result. $\overleftarrow{h}_t$A denotes the reverse learning result.

The gear system shown in Figure 3 is a dual transmission gear system with two clutches, an inner transmission shaft, an outer transmission shaft, and six different speed gears. In the working process of the gear system, the appearance of certain faults can cause the transmission to stop working, therefore, the detection of faults in the gear system of the transmission is an important research direction for automobile safety. The vibration signal generated by

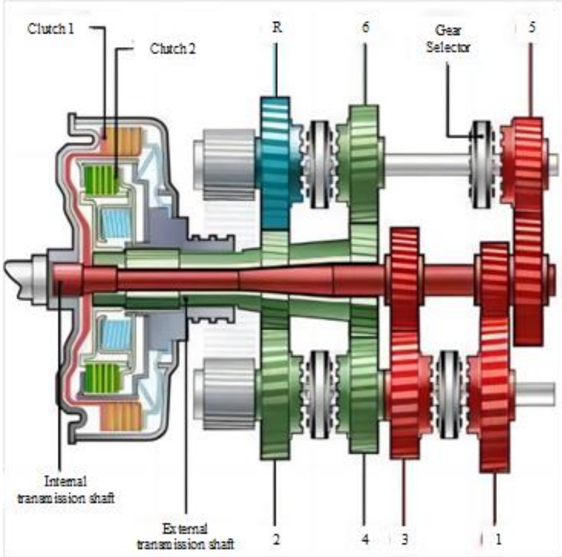

Fig. 3. Gear system structure

the gears during the gearing process is non-stationary. This non-stationary vibration signal produces a great disturbance to the accurate diagnosis of gear failure. Since the gear's vibration system is nonlinear, study on its dynamics must simplify its dynamics equation. And the simplified dynamics equation is shown in equation (10).

$$M_r\ddot{x} + C\ddot{x} + k(t)x = k(t)E_1 + k(t)E_2 t \qquad (10)$$

In equation (10), M_r denotes the equivalent mass of the gear pair and x denotes the relative displacement on the gear meshing line. C denotes the damping of the gears when they mesh, $k(t)$ denotes the gear mesh stiffness shape. E_1 denotes the average static elastic deformation of the gear after being loaded. $E_2 x$ denotes the relative displacement between gears that mesh with each other as a result of errors or failures that may occur in the gears. The left part of equation (10) represents the vibration characteristics of the gear in the working state, and the right part represents the dynamic loads of the gear. The dynamic loads of the gear system include the inherent vibration of meshing, and the vibration caused by the gear stiffness and gear failure, and the second vibration can be explained for various failure conditions in the gear. Since the meshing stiffness of the gears in a gear system varies with the meshing rotation of the gears, equation (11) illustrates that the meshing frequency of the gear system is equal to the frequency of change of the meshing stiffness.

$$f_z = \frac{nOz}{60} \qquad (11)$$

In equation (11), f_z denotes the meshing frequency of the gear and n denotes the harmonics. O denotes the revolutions of the shaft where the gear is located, and z denotes the number of gear teeth. Equation (12) illustrates that the gear's vibration signal is made up of the meshing frequency and the high harmonics.

$$x(t) = \sum_{p=0}^{P} A_p \cos\left(2\pi n f_z + \phi_p\right) \qquad (12)$$

In equation (12), denotes the total number of gear meshing frequency orders, and A_p denotes the amplitude of the pth order gear meshing frequency. ϕ_p denotes the initial phase of the pth order meshing frequency. The fault produced by the gear is the excitation source of this type of vibration, which is based on the rotation period of the gear shaft as the period. Therefore, the vibration information will contain the rotation frequency and multiplicity of the faulty gear. When the fault occurs, not only vibration will be generated, but also shocks will be generated during the meshing process, causing the signal to generate side bands, at which point, equation (12) will be rewritten as equation (13).

$$x(t) = \sum_{p=0}^{P} A_p \times \left[1 + a_p(t)\right] \cos\left(2\pi n f_z + \phi_p + b_p(t)\right) \qquad (13)$$

In equation (13), $a_p(t)$ denotes the amplitude modulation function of the pth order engagement frequency. $b_p(t)$ denotes the frequency modulation function of the pth order meshing frequency. The modulation frequency includes the station east frequency of the shaft where the faulty gear is located and the multiplicity, therefore, equation (13) can be transformed into equation (14).

$$x(t) - \sum_{p=0}^{P} A_p \times [1 + \sum_{m=0}^{M} B_m \cos(2\pi n f_n t)] \cos(2\pi n f_n + \sum_{m=0}^{M} G_m \sin(2\pi n f_n t)) \qquad (14)$$

In equation (14), M denotes the maximum modulation order. B_m denotes the amplitude modulation coefficient of the mth order rotation frequency modulation, and $\mathrm{G_m}$ denotes the frequency modulation coefficient of the mth order rotation frequency modulation. $\mathrm{f_n}$ denotes the rotation frequency of the rotating shaft, and its calculation is shown in equation (15).

$$\mathrm{f_z} = \mathrm{Zf_n} \qquad (15)$$

In the previous paper, two network structures, SDEA and Bi-GRU, are proposed, and the study combines them to construct a hybrid SDEA-Bi-GRU network for transmission gear fault diagnosis. Model training and model testing comprise the two main components of this network's overall architecture, which is seen in Figure 4.

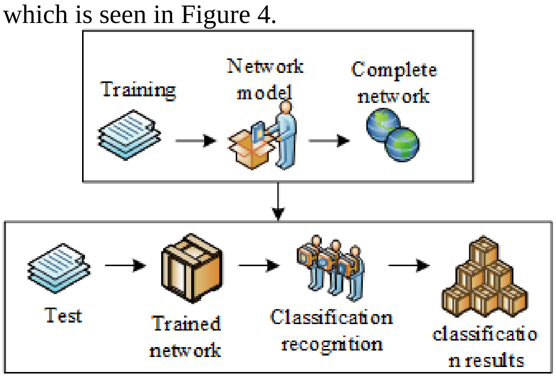

Fig. 4. Basic framework of fault diagnosis model

Based on the basic framework of the model, the study redesigned the network structure of the SDEA-Bi-GRU model. The hybrid network structure consists of three parts, which are SDEA structure, Bi-GRU structure and Softmax classifier structure. When performing fault diagnosis, the time-domain signal of the transmission gear system is used as the input data to the SDEA structure, in which noise reduction is performed. The signal is then fed into the Bi-GRU in order to extract the signal's fault features. Ultimately, the fault signal is categorized using the Softmax classifier, allowing the diagnosis of the gear failure of electric vehicle transmission to be finished. Figure 5 depicts the precise architecture of the hybrid network.

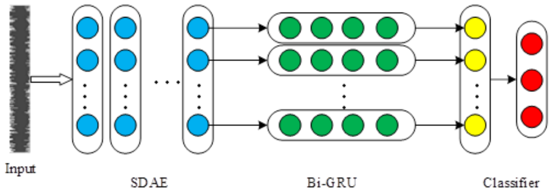

Fig. 5. Hybrid network structure

During the training process of hybrid networks, it is necessary to prevent neural networks from overfitting. Dropout technique is a common regularization technique used to reduce the occurrence of overfitting in neural networks. Dropout has a probability that the output of each neuron will be randomly discarded during the training process. This operation forces the neural network to learn redundant features and reduces the collaborative dependency between neurons, improving the generalization performance of the network. And Dropout can randomly disconnect connections during training and then keep all connections for prediction, reducing the neural network's dependence on colorful neurons thus preventing the hybrid network from overfitting phenomenon during training. Figure 6 depicts the Dropout network's structure.

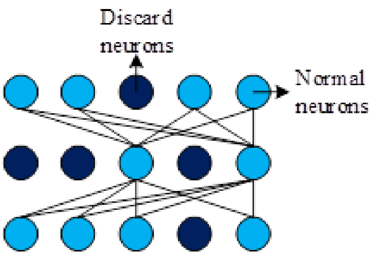

Fig. 6. Dropout network structure

3.2. SDEA-Bi-GRU based gear fault diagnosis

Transmission is a common basic component in automobiles with high ratios and compact structural design, it is very common in industrial applications. A transmission gear system is a mechanical system capable of varying the ratio between the drive wheels and the engine to provide different speeds and torque outputs. The main component of the gear system is a series of gears, which work in conjunction with devices such as drive shafts, main shafts and clutches. The structure of the transmission gear system is shown in Figure 3.

4. EXPERIMENTAL VALIDATION OF THE EFFECT OF SDEA-BI-GRU MODELING

The study constructed a hybrid SDEA-Bi-GRU neural network and used the network for transmission gear fault diagnosis of electric vehicle. The main content of this chapter is the verification of the practical effect of the model, which is divided into three parts. The model's training results are analyzed in the second part, the experimental environment and parameters are set, and the model's impact on practical application is examined in the third part.

4.1. Experimental environment and parameter settings

All the experiments of the study are completed using the equipment at the time of the experiment, the operating system is windows 7 professional, the CPU is Intel(R) Core(TM) i5-4460 CPU @ 3.20GHz 3.20 GHz, the RAM is 16GB, and all the data analyzing software is carried out on the MATLAB platform. In addition to the basic experimental environment, the study also builds a fault simulation test bed, which is shown as a 3D model in Figure 7.

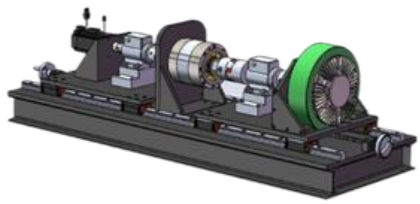

Fig. 7. Gear fault simulation test bench

After completing the construction of the experimental environment, the study conducts training tests on SDEA and Bi-GRU. In the training, the input noise ratio of the SDEA structure is 0.3, the discard rate of the network structure is set to 0.1, the learning rate is set to 0.001, the maximum iterations are 600, and the decay rate is 0.95 and 0.99. The training results are shown in Figure 8.

Figure 8(a) illustrates how the neurons affects SDEA performance. The diagnostic time of SDEA for fault occurrence increases with the neurons; for example, when the neurons rises from 80 to 200, the diagnostic time of SDEA increases by around 50 minutes overall. The highest score of 94.8% is reached by SDEA's diagnostic accuracy when the buried layer has 180 neurons. The SDEA structure's diagnostic accuracy rises with the neurons when there are fewer than 180 neurons. When the neurons exceed 180, the accuracy of the diagnosis declines as the neurons rises. It takes 37 minutes to diagnose SDEA when there are 180 neurons in the brain. Figure 8(b) illustrates how the quantity of neurons affects Bi-GRU performance. Both the changes in diagnostic time and diagnostic accuracy are similar to Figure 8(a). The diagnosis accuracy of Bi-GRU reaches the maximum value of 98.0% when the number of neurons is 160, and at this time, the diagnosis of Bi-GRU takes 45 min. The study determined that there should be 180 neurons in the hidden layer of the SDEA structure and 160 neurons in the hidden layer of the Bi-GRU structure, respectively, based on the training results.

4.2. Fault diagnosis results for SDEA-Bi-GRU models

The hybrid model constructed by the study is proposed based on SDEA and Bi-GRU, therefore, the study compares the feature extraction ability of SDEA and SDEA-BiGRU for gear failure signals, and the results are shown in Figure 9.

Figure 9(a) shows the feature extraction capability of the SDEA structure for the gear states in 6. There is a crossover between the scatter region of normal gears and mildly cracked gears, a crossover between mildly cracked and heavily cracked, a crossover between heavily cracked and broken teeth, and a crossover between broken teeth and tooth wear. In the gear failure states extracted from the SDEA structure, there is a serious crossover between the different fault feature signals and the respective scatter regions are more dispersed. Figure 9(b) shows the feature extraction capability of SDEA-Bi-GRU for six gear states. The model has a better extraction effect on gear failure states, and there is only a crossover between normal gears and mild cracks, and there is no crossover for the rest of the various types of faults, and the regional distribution of the various types of faults is more concentrated. The extraction effect of SDEA-Bi-GRU on gear failure signal features is much better than that of SDEA structure. In the simulation experiment, the study controls the speed of the gearbox so that the intensity of the vibration signal

is reduced from 70 Hz to 30 Hz. And 12 different sample sets are formulated in accordance with each 10 Hz drop as a sample set, which is divided into four sample sets of D, B, A and C. Table 1 presents the findings of a comparison of the diagnostic procedures' accuracy.

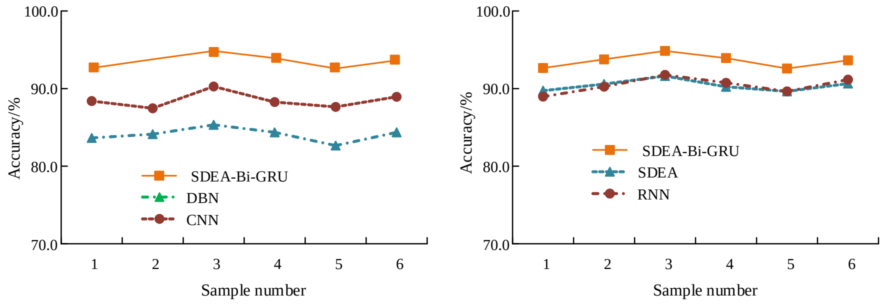

Fig. 10. Comparison of diagnostic accuracy for imbalanced samples

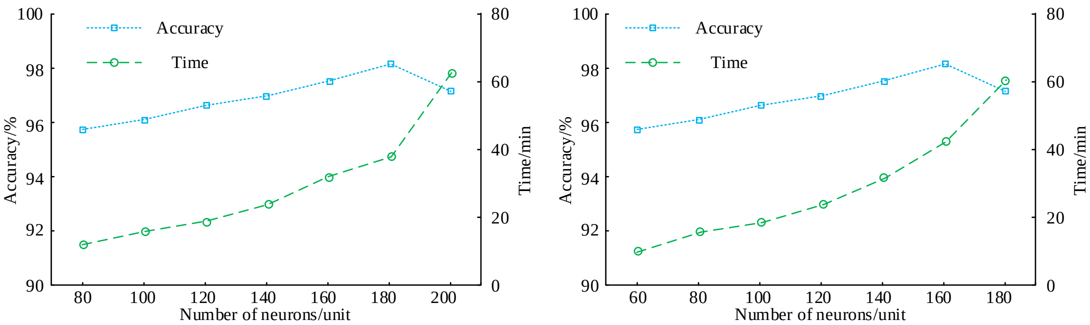

(a) SDAE (b) Bi-GRU

Fig. 8. Effect of neuron number on the performance of SDEA and Bi-GRU

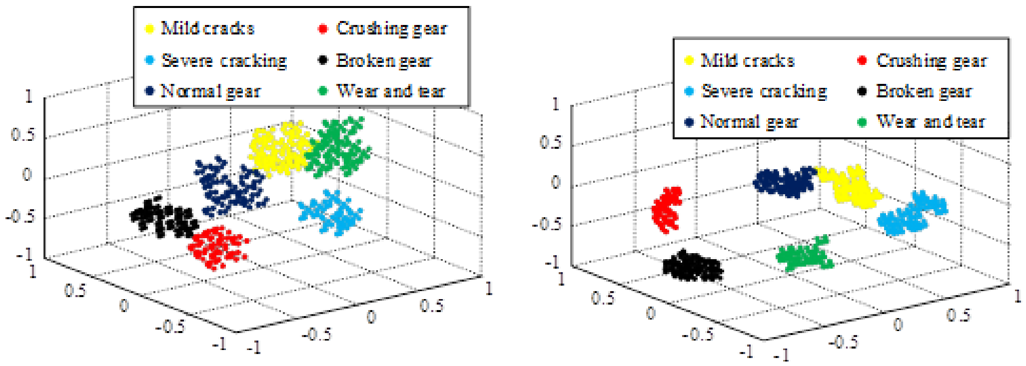

(a) SDEA (b) SDEA-Bi-GRU

Fig. 9. Feature extraction capabilities of different network structures

Table 1. Comparison of diagnostic effects of different methods

Sample num.	SDEA-Bi-GRU (%)	RNN (%)	CNN (%)	SDEA (%)	DBN (%)
1	97.98	94.65	89.37	79.63	76.54
2	86.54	91.35	78.64	75.62	71.62
3	88.69	84.35	88.66	74.89	75.54
4	86.94	79.64	83.15	74.32	74.39
5	96.34	84.56	78.64	71.84	73.34
6	92.51	86.54	75.63	65.36	68.94
7	94.56	86.34	74.31	68.72	62.38
8	96.66	88.92	88.64	78.35	61.57
9	92.36	89.65	85.61	77.51	69.66
10	89.67	87.61	84.67	74.94	63.54
11	88.97	82.36	86.34	76.53	68.68
12	95.64	84.65	82.79	75.18	69.75

CNN, deep belief network (DBN), and RNN are all common fault diagnosis networks. Table 1 illustrates how utilizing distinct sample sets for the model's training and sample sets will significantly affect the model's diagnostic accuracy. All the algorithms have the highest accuracy in sample set 1. The highest diagnostic accuracy is 76.54% for DBN, 89.37% for CNN, 94.65% for RNN, 79.63% for SDEA, and 97.98% for SDEA-Bi-GRU. The proposed algorithm of the study is the most effective for fault diagnosis of gears. To simulate the actual situation as much as possible, the study adjusted the ratio of normal gears to faulty gears in the sample set. And Figure 10 displays the test findings.

Figure 10(a) shows the comparison of the accuracy of DBN and CNN with SDEA-Bi-GRU. CNN's diagnostic accuracy in unbalanced samples is at a better level, with a maximum diagnostic accuracy of 90.27%, while DBN's diagnostic accuracy is at a lower level, with a maximum of only 85.33%. SDEA-Bi-GRU has a diagnostic accuracy of 94.86%, which is much higher than the other two algorithms' accuracy in unbalanced samples. Figure 10(b) shows the accuracy comparison of SDAE and RNN with SDEA-Bi-GRU. The highest diagnosis accuracy of both SDAE and RNN can reach more than 90%, but it is still lower than the fault diagnosis accuracy of SDEA-Bi-GRU. In unbalanced samples, the diagnosis accuracy of SDEA-Bi-GRU model for transmission gear failure is also better than the rest of the algorithms. Because the signal-to-noise ratio (SNR) also has a significant impact on fault diagnosis, the study also examines the diagnosis accuracy of SVM using SDEA-Bi-GRU and back propagation (BP) neural networks under various SNRs. The findings are displayed in Figure 11.

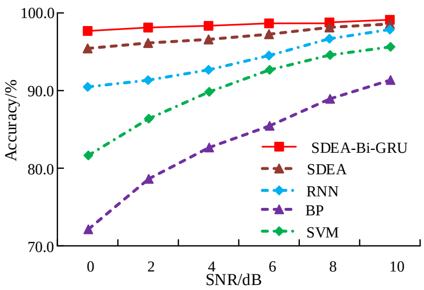

Fig. 11. The impact of signal-to-noise ratio on algorithm performance

In Figure 11, the accuracy of the algorithms increases as the SNR increases, with the BP Neural Network showing the greatest improvement in accuracy and the SDEA Bi-GRU showing the least change in accuracy. The fault diagnosis accuracy of the BP neural network is 72.13%, the fault diagnosis accuracy of the SVM is 81.65%, the fault diagnosis accuracy of the RNN is 90.47%, the fault diagnosis accuracy of the SDEA is 95.43%, and the fault diagnosis accuracy of the SDEA-Bi-GRU is 97.68% when the SNR is 0 dB. At a SNR of 10 dB, the fault diagnosis accuracy for BP neural networks is 93.76%, the fault diagnosis accuracy for SVMs is 95.63%, the fault diagnosis accuracy for RNNs is 97.86%, the fault diagnosis accuracy for SDEA is 98.63%, and the fault diagnosis accuracy for SDEA-Bi-GRU is 99.37%. The fault diagnosis accuracy for BP neural networks increases by a total of 21.63%, the fault diagnosis accuracy for SVMs increases by a total of 13.98%, the fault diagnosis accuracy of RNN is 7.39%, the fault diagnosis accuracy of SDEA is 3.20%, and the fault diagnosis accuracy of SDEA-Bi-GRU is 1.69%. The SNR has the least effect on SDEA-Bi-GRU and the algorithm has the highest fault diagnosis accuracy.

5. CONCLUSION

Aiming at the fault diagnosis problem of electric vehicle transmission, the study successfully developed a hybrid algorithm based on SDEA and Bi-GRU, which is used to enhance the diagnosis of gear failure of electric vehicle transmission. The SDEA-Bi-GRU algorithm enhances the accuracy and efficiency of the gear fault diagnosis of gearboxes by efficiently combining the feature extraction capability of the denoising selfencoder with the highly efficient time-series analyzing capability of the Bi-GRU. The experimental results demonstrated that the SDEA-Bi-GRU algorithm was able to accurately extract the key features when dealing with complex transmission signals, and the hybrid algorithm extracted the fault signal feature regions that were concentrated and had less crossover between the regions. The hybrid algorithm achieved the highest fault diagnosis accuracy of 97.98% in balanced samples and 99.37% in unbalanced samples, and the remaining algorithms achieved the highest accuracy of 94.65% in balanced samples and 98.63% in unbalanced samples, and the hybrid algorithm had the best diagnostic effect on the faults. Additionally, the SNR of the input signal had minimal effect on the hybrid algorithm. As the SNR increased, the diagnostic accuracy of the hybrid algorithm fluctuated only 1.69%, while the rest of the algorithms fluctuated at least 3.20%. The hybrid algorithm demonstrated significant advantages over traditional diagnostic methods and other machine learning algorithms in terms of fault diagnosis of electric vehicle transmission. The study improves the efficiency and accuracy of fault diagnosis of electric vehicle transmissions and provides technical support for the safe operation and maintenance of electric vehicles. Future work will focus on optimizing the algorithm's performance, expanding its application to more electric vehicle critical components, and exploring its practicality in real industrial environments.

Source of funding: *The research is supported by: Huai'an Science and Technology Support Program (Industry) Project: Design and Analysis of Gear System of Pure Electric Vehicle Transmission (No. HAB202161); Jiangsu Qinglan Project (2021).*

Author contributions: *research concept and design, L.Z.; Collection and/or assembly of data, L.Z., T.W.; Data analysis and interpretation, T.W.; Writing the article, L.Z.; Critical revision of the article, T.W.; Final approval of the article, T.W.*

Declaration of competing interest: *The authors declare that they have no known competing financial interests or personal relationships that could have appeared to influence the work reported in this paper.*

REFERENCES

1. Wang Z, Song C, Zhang L, Zhao Y, Liu P, Dorrell D G. A data-driven method for battery charging capacity abnormality diagnosis in electric vehicle applications. IEEE Transactions on Transportation Electrification 2021; 8(1): 990-999. https://doi.org/10.1109/TTE.2021.3117841
2. Kong W, Luo Y, Qin Z, Qi Y, Lian X. Comprehensive fault diagnosis and fault-tolerant protection of in-vehicle intelligent electric power supply network. IEEE Transactions on Vehicular Technology 2019; 68(11): 10453-10464. https://doi.org/10.1109/TVT.2019.2921784.
3. Abdelli K, Grießer H, Tropschug C, Pachnicke S. Optical fiber fault detection and localization in a noisy OTDR trace based on denoising convolutional autoencoder and bidirectional long short-term memory. Journal of Lightwave Technology 2022; 40(8): 2254-2264. https://doi.org/10.48550/arXiv.2203.12604.
4. Wang Z, Song C, Zhang L, Zhao Y, Liu P, Dorrell D G. A data-driven method for battery charging capacity abnormality diagnosis in electric vehicle applications. IEEE Transactions on Transportation Electrification 2021; 8(1): 990-999. https://doi.org/10.1109/TTE.2021.3117841.
5. Li D, Zhang Z, Liu P, Wang Z, Zhang L. Battery fault diagnosis for electric vehicles based on voltage abnormality by combining the long short-term memory neural network and the equivalent circuit model. IEEE Transactions on Power Electronics 2020; 36(2): 1303-1315. https://doi.org/10.1109/TPEL.2020.3008194.
6. Gan N, Sun Z, Zhang Z, Xu S, Liu P, Qin Z. Data-driven fault diagnosis of lithium-ion battery overdischarge in electric vehicles. IEEE Transactions on Power Electronics 2021; 37(4): 4575-4588. https://doi.org/10.1109/TPEL.2021.3121701.
7. Wang X, Lu S, Chen K, Wang Q, Zhang S. Bearing fault diagnosis of switched reluctance motor in electric vehicle powertrain via multisensor data fusion. IEEE Transactions on Industrial Informatics 2021; 18(4): 2452-2464. https://doi.org/10.1109/TII.2021.3095086.
8. Long R, Yu Q, Shen W, Lin C, Sun F. A sensor fault diagnosis method for a lithium-ion battery pack in electric vehicles. IEEE Transactions on Power Electronics 2019; 34(10): 9709-9718. https://doi.org/10.1109/TPEL.2019.2893622.
9. Deng F, Bian Y, Zheng H. Fault diagnosis for electric vehicle lithium batteries using a multi-classification support vector machine. Electrical Engineering 2022; 104(3): 1831-1837. https://doi.org/10.1007/s00202-021-01426-y.
10. Jia N, Cheng Y, Liu Y, Tian Y. Intelligent fault diagnosis of rotating machines based on wavelet time-frequency diagram and optimized stacked denoising auto-encoder. IEEE Sensors Journal 2022; 22(17): 17139-17150. https://doi.org/10.1109/JSEN.2022.3193943.
11. Che C, Wang H, Ni X, Fu Q. Intelligent fault diagnosis method of rolling bearing based on stacked denoising autoencoder and convolutional neural network. Industrial Lubrication and Tribology 2020; 72(7): 947-953. https://doi.org/10.1108/ILT-11-2019-0496.
12. Fu B, Yuan W, Cui X, Yu T, Zhao X, Li C. Correlation analysis and augmentation of samples for a bidirectional gate recurrent unit network for the remaining useful life prediction of bearings. IEEE sensors journal 2020; 21(6): 7989-8001. https://doi.org/10.1109/JSEN.2020.3046653
13. Liu H, Liu Z, Jia W, Zhang D, Tan J. A novel imbalanced data classification method based on weakly supervised learning for fault diagnosis. IEEE Transactions on Industrial Informatics 2021; 18(3): 1583-1593. https://doi.org/10.1109/TII.2021.3084132.
14. Pal S, Roy A, Shivakumara P, Pal U. Adapting a Swin Transformer for License Plate Number and Text Detection in Drone Images. Artificial Intelligence and Applications 2023; 1(3): 145-154. http://dx.doi.org/10.47852/bonviewAIA3202549
15. Wang T, Luo H, Zeng X, Yu Z, Liu A, Sangaiah A K. Mobility based trust evaluation for heterogeneous electric vehicles network in smart cities. IEEE Transactions on Intelligent Transportation Systems 2020; 22(3): 1797-1806. https://doi.org/10.1109/TITS.2020.2997377
16. Liu C, Chau K T, Lee CHT, Song Z. A critical review of advanced electric machines and control strategies for electric vehicles. Proceedings of the IEEE 2020; 109(6): 1004-1028. https://doi.org/10.1109/JPROC.2020.3041417.
17. Yang D, Pang Y, Zhou B, Li K. Fault diagnosis for energy internet using correlation processing-based

convolutional neural networks. IEEE Transactions on Systems, Man, and Cybernetics: Systems 2019; 49(8): 1739-1748. https://doi.org/10.1109/TSMC.2019.2919940.
18. Dhaya DR, Kanthavel DR. A wireless collision detection on transmission poles through IoT technology. Journal of Trends in Computer Science and Smart Technology 2020; 2(3): 165-172. http://dx.doi.org/10.36548/jtcsst.2020.3.006.
19. Racewicz S, Kazimierczuk P, Kolator B, Olszewski A. Use of 3 kW BLDC motor for light two-wheeled electric vehicle construction, IOP Conference Series: Materials Science and Engineering, 2018;421:042067. https://iopscience.iop.org/article/10.1088/1757-899X/421/4/042067.

Linlin ZHAO
was born in February 1982. She obtained Bachelor's degree in Mechanical Design and Automation from Shandong University of Light Industry in 2004 and her Master's degree in Mechanical Engineering from Nanjing University of Aeronautics and Astronautics in 2007. She got her PhD in Mechanical Engineering from Nanjing Forestry University in 2018. Her research interests include mechanical optimization design, intelligent manufacturing, and more. She works at Jiangsu Vocational and Technical College of Finance and Economics since 2007. She published over 20 academic papers, invented more than 10 utility model patents and presided over 2 provincial-level projects, 4 or more municipal level projects.
e-mail: zhaolinlin108@126.com

Tao WU
born in December 1981. He got his bachelor's degree of Mechanical Design, Manufacturing, and Automation from Shandong University of Light Industry in 2004 and master's degree of Mechanical Engineering from Nanjing University of Aeronautics and Astronautics in 2014. He works as full-time teacher at Jiangsu Vocational and Technical College of Finance and Economics since August 2020. He published 3 papers, participated in the compilation of 1 textbook and obtained 2 utility model patents.
e-mail: wutao312@126.com